

Soft Matter

Accepted Manuscript



This is an *Accepted Manuscript*, which has been through the Royal Society of Chemistry peer review process and has been accepted for publication.

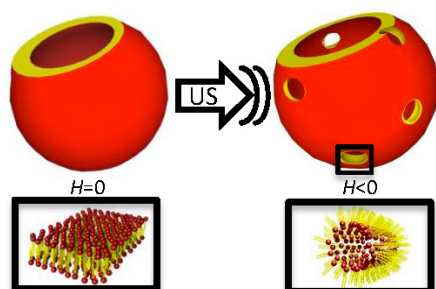
Accepted Manuscripts are published online shortly after acceptance, before technical editing, formatting and proof reading. Using this free service, authors can make their results available to the community, in citable form, before we publish the edited article. We will replace this *Accepted Manuscript* with the edited and formatted *Advance Article* as soon as it is available.

You can find more information about *Accepted Manuscripts* in the [Information for Authors](#).

Please note that technical editing may introduce minor changes to the text and/or graphics, which may alter content. The journal's standard [Terms & Conditions](#) and the [Ethical guidelines](#) still apply. In no event shall the Royal Society of Chemistry be held responsible for any errors or omissions in this *Accepted Manuscript* or any consequences arising from the use of any information it contains.

Table of contents entry

We investigate liposome membrane restructuring induced by ultrasound exposure. Ultrasound induces membrane thinning and when non-lamellar lipids are present there is a topological restructuring from lamellar- L_α to reversed hexagonal- H_{II} phases.



Role of lipid polymorphism in acoustically sensitive liposomes

*Minjee Kang, Grace Huang, and Cecilia Leal**

Department of Materials Science and Engineering, University of Illinois at Urbana-Champaign,
Urbana, IL 61801

Abstract

Ultrasound (US) triggered drug release is a promising drug delivery method that allows ex-vivo modulation of treatment intensity and duration. This method relies on the synergistic interaction between rupture of sonosensitive particles and enhanced plasma membrane permeability. Conventional liposomal systems where the drug passively diffuses through the membrane show virtually no response to acoustic energy. One method to activate drug transport is to induce a topological restructuring of the lipid membrane (zero intrinsic curvature, $H = 0$) by puncturing pores ($H < 0$) through which the drug can readily leak out from the interior of the liposomes. In this work we demonstrate strategies to lower the energy cost of creating such membrane defects by introducing lipid molecules with molecular shapes prone to self-assemble into non-lamellar (negative intrinsic curvature, $H < 0$) structures. All formulations investigated comprise the relevant components typically required for delivery applications such as stealth moieties, cholesterol, and phospholipids. Small Angle X-ray Scattering studies of a number of lipid systems at increasing amounts of phosphatidylethanolamine (PE) phospholipids reveal that membranes without PE respond to ultrasound by thinning *ca.* 10 Å, which concomitantly lowers the bending rigidity quadratically in addition to increasing the passive drug permeability. However, at the appropriate PE content the lipid systems display a classic lamellar structure ($H = 0$) that undergoes a topological transformation after ultrasound exposure into lipid tubes of the reversed type ($H < 0$) packed in a 2D hexagonal array. At the dilute regime, Fluorescence Microscopy of Giant Unilamellar Vesicles comprising DOPE also experience ultrasound induced restructuring that can be modulated by DOPE content. In general, smaller vesicles of diverse shape connect and form into a “pearl-necklace” configuration. We argue that the inclusion of DOPE within the GUV membrane may result in curvature-driven lipid sorting, providing the system with local membrane instabilities that drive vesicle pearling when exposed to ultrasound.

Introduction

Traditional drug delivery systems often fail to deliver the required drug load at an optimal spatiotemporal setting. Presently, a wide number of materials have been designed to encapsulate adequate drug dosages that are released in response to an external stimulus.^{1, 2} Ultrasound (US) represent an effective method for attaining triggered drug release via thermal and/or mechanical effects that transiently disrupt the drug carrier without harming surrounding healthy tissue.^{3, 4} In addition to being non-invasive, ultrasound does not generate ionizing radiations and is easily regulated with respect to tissue penetration depth by tuning of frequency, duty cycle, and exposure time. Nearly all successful US responsive drug capsules involve gas-containing particles which have a short lifetime in addition to being too big to be viable carriers for efficient extravasation at tumor sites.⁵ Some strategies have been developed to overcome this issue including the development of nanoscale emulsions functionalized with aptamers⁶ and liposomes containing air pockets⁷⁻¹¹ to provide sonosensitivity to the drug carrier. In fact, liposomes are an extremely important class of drug carriers. They are able to incorporate high loads of both water soluble and hydrophobic drugs, their sizes are easily controllable, and their compositions can be tailored to respond to several stimuli such as pH, temperature, and light.² Traditional liposomes are typically not very sensitive to acoustic energy, but there have been efforts¹² to use conventional formulations for the purpose of low frequency ultrasound release. Liposome drug delivery in response to triggers relies on some sort of membrane phase transition. This can involve transformations of lipid hydrophobic tails from crystalline to liquid crystalline, leading to a rapid increase in drug permeability and/or topological restructuring such as the formation of pores. Indeed, pH driven delivery is based on the latter concept where the liposome lamellar bilayer transforms into a reversed hexagonal phase in acidic environments.¹³ Generally speaking, membrane restructuring that involves a lamellar to a non-lamellar phase transition is the most efficient method to trigger release from lipid systems.^{14, 15}

In this work, we investigate the mechanisms associated with topological restructuring of liposomal membranes in response to ultrasound. Leal and co-workers first suggested that sonosensitivity of liposomes can be achieved by the inclusion of instabilities in the lipid membrane

such as lowering of bending rigidity by the incorporation of medium chain length alcohols (hexanol) or by inducing local membrane curvature stress with the addition of conically shaped lipids such as phosphoethanolamines (PE).^{16, 17} In these studies, a number of classic liposomal formulations comprising phosphatidylcholines (PC), cholesterol, and polyethylene glycol covalently linked to PE lipids were doped with increasing amounts of different types of PE molecules and/or with minor levels of hexanol. The main finding was that hexanol as well as PE lipids induce local stresses (membrane thinning and curvature) within the core liposomal membrane made of PC lipids leading to an increase in sonosensitivity and drug release. In fact, low-frequency ultrasounds have been used to successfully trigger siRNA delivery to skin melanocytic lesions using liposomes comprising dioleoylphosphoethanolamine (DOPE).¹⁸ The exact mechanism underlying liposome membrane sonosensitivity is not fully well established but it is considered that inertial cavitation consisting of the collapse of air bubbles near the surface of the cells or liposomes is able to induce pores in the lipid membrane.^{19, 20} Lipids with negative mean spontaneous curvature have a preference to self-assemble into so-called reversed structures where the bulky nature of the hydrophobic part of the lipid imposes an orientation towards the aqueous phase. Long chain unsaturated PE molecules such as DOPE belong to this category of lipids. When dispersed in water, DOPE molecules spontaneously form reversed hexagonal structures (H_{II}) for temperatures above 10 °C (below 10 °C the bilayer phase is preferred).²¹ The conditions for which a DOPE forms H_{II} phases can be modulated by changing the degree of unsaturation in the chain and also the temperature.²² This particular membrane transformation has important implications for drug delivery because the H_{II} transition is initiated by the formation of holes in the lipid bilayer²³ that are large enough (*ca.* 3 nm in diameter) for most drugs to penetrate out. Other classes of phase transitions can have a similar effect as long as they involve a topological change in membrane structure. As shown by Lin and Thomas,²⁴ a formulation can be made more US responsive by including lipids that are prone to form micellar aggregates. Our hypothesis is that generally, the inclusion of appropriate amounts of “non-lamellar” lipid molecules within the liposome membrane is a promising approach to introduce local

instabilities. These instabilities are not enough to disturb membrane integrity before stimuli is applied; but they respond once the trigger is on and heal once the stimulus is turned off.

Even though the drug release profile as a function of sonication time is relatively easy to access,²⁵ the detection of transient restructuring from lamellar to non-lamellar phases as a response to ultrasound exposure is a rather unexplored subject. To our knowledge, this subject has not been demonstrated to date. In our work, we used a powerful combination of Small Angle X-ray Scattering (SAXS) techniques and Fluorescence Microscopy (FM) to investigate the membrane structure at increasing amounts of DOPE before and after ultrasound exposure in concentrated and diluted systems. We present clear evidence that when an appropriate amount of DOPE is selected, liposome membranes experience restructuring in response to applied acoustic energy including the topological lamellar-hexagonal phase transition.

Materials and Methods

Materials

1,2-Dioleoyl-sn-glycero-3-phosphoethanolamine (DOPE), 1,2-dioleoyl-sn-glycero-3-phosphocholine (DOPC), 1,2-dioleoyl-sn-glycero-3-phosphoethanolamine-N-[methoxy(polyethylene glycol)-2000] (DOPE-PEG2000), Cholesterol (purity >98%) were purchased from Avanti Polar Lipids (Alabaster, AL). All lipids were used without further purification. The fluorescent lipid, 1,2-dihexadecanoyl-sn-glycero-3-phosphoethanolamine, triethylammonium salt (Texas Red® DHPE) was purchased from Life Technologies (Grand Island, NY). Glycerol, HEPES and sucrose were purchased from Sigma-Aldrich (St. Louis, MO). The liposomes were passively loaded with a drug model substance calcein. Calcein was purchased by Sigma-Aldrich and used to prepare a 50 mM stock solution in HEPES (10 mM). Triton X was obtained by Sigma-Aldrich and used as received.

Small Angle X-ray Scattering (SAXS)

Liposomes were prepared using the thin film hydration method.²⁶ In summary, stock solutions of DOPC, DOPE, DOPE-PEG and Cholesterol dissolved in chloroform (25 mg/ml) were mixed at the desired mole ratio. The mixtures were dried under N_2 , desiccated under vacuum for overnight, and hydrated with Millipore water at 50°C for 24 h to a final lipid concentration of 1 M. Liposomes were prepared in 1.5 mm quartz X-ray capillaries (Hilgenberg Glas, Germany). SAXS experiments were conducted in a home built (Forvis Technologies, Santa Barbara) equipment composed of a Xenocs GeniX3D CuK α Ultra Low Divergence X-ray source (1.54Å / 8 keV), with a divergence of ~ 1.3 mrad. The 2D diffraction data were radially averaged upon acquisition on a Pilatus 300K 20 Hz hybrid pixel Detector (Dectris) and integrated using FIT2D software (<http://www.esrf.eu/computing/scientific/FIT2D>) from ESRF. The reference samples without DOPE were measured by Synchrotron SAXS at the Stanford Synchrotron Radiation Light source, beamline 4-2. The 2D powder diffraction data was acquired on a MX-225 CCD detector (Rayonics).

Fluorescence Microscopy

Giant unilamellar vesicles (GUVs) were prepared by the electroformation method.²⁷ Briefly, mixtures of DOPC, DOPE, DOPE-PEG, Cholesterol, and fluorescent label Texas Red® DHPE (1 mol%) were dissolved in a 2:1 (v/v) chloroform/methanol mixture and deposited onto clean ITO-coated glass (30 μ l at 10 mg/ml). The cast film was dried under vacuum for an hour and then filled with ~2.7 ml of aqueous buffer containing 100 mM sucrose in a 2:1 (v/v) glycerol/water mixture. The two ITO glasses were secured together tightly by rubber bands. An AC voltage of 10V (2V/mm) at a frequency of 7Hz was applied between the electrodes from a function generator (Hewlett Packard). After 2 hours, the function generator was turned off and the vesicles were let to relax overnight in the preparation chamber and then were drawn out carefully. Images of the GUVs were obtained using a home-built epifluorescence imaging microscope equipped with a Nd:YVO₄ laser of 532 nm excitation wavelength.

Sonication

To test the effect of ultrasound, samples were indirectly sonicated via a sonicator equipped with a cup horn attachment (Qsonica) at controlled temperature (25°C) using a chiller (Fisher Scientific). The ultrasound frequency was 20 kHz and exposure time was 10 min. The average energy applied to liposomes during sonication is 70 kJ. Pressure measurements were conducted with a Bruel and Kjaer hydrophone type 8103. At 20% amplitude, acoustic pressure measurements in the sample chamber gave 430 kPa (pk-pk).

The release assessment of calcein is based on the following well-established methodology: Intact liposomes containing calcein will display low fluorescence intensity due to self-quenching caused by the high intraliposomal concentration of material. Ultrasound mediated release of material into the extraliposomal phase can be determined by a marked increase in fluorescence intensity due to a reduced quenching effect. The following equation is used for release quantification:

$$\% \text{ release} = \frac{(F_u - F_b)}{(F_T - F_b)} \times 100$$

Where F_b and F_u are, respectively, the fluorescence intensities of the liposome sample before and after ultrasound application. F_T is the fluorescence intensity of the liposome sample after solubilization with surfactant (Triton-X 100). Studies have shown that the solubilization step must be performed at high temperature, above the phase transition temperature of the phospholipid mixture.

Fluorescence measurements were carried out in a The Horiba FluoroMax[®] 4 spectrometer equipped with 150 W xenon, continuous output, ozone-free lamp. The excitation monochromator has an optical range of 220 – 600 nm and the emission monochromator has an optical range of 290 – 850 nm blazed at 500 nm.

Results

In this work we intend to describe the lipid membrane properties that control the sensitivity of liposomes to ultrasound (US) energy. Leal and coworkers¹⁷ firstly observed that the incorporation of phosphoethanolamine lipids (PE) in model drug loaded stealth liposomes resulted in more efficient drug release as triggered by US energy when compared to parent phosphocholine (PC) systems. Pure PE lipid structures are known for self-assembling into non-lamellar aggregates of negative preferred mean curvature (H) when compared to PC lipids that typically form lamellar phases of $H = 0$. It was suggested that PE lipids introduce “non-lamellar” structural instabilities in the liposome membrane that locally help nucleating transient pores that facilitate drug escape. A later report confirmed that 1,2-dioleoyl-*sn*-glycero-3-phosphoethanolamine (DOPE)-containing liposomes showed nine times more efficient Doxorubicin release for the same US exposure time and frequency, compared to reference PC-based liposomes.²⁵ Here we also performed a model drug (calcein) leakage assay on DOPE-containing liposomes and reference liposomes to check the drug release profiles as a function of US exposure time. Specifically, two formulations were prepared containing: i) DOPE 62 mole%, DOPC 15 mole %, Cholesterol 20 mole %, and DOPE-P3G 3 mole % and ii) DOPC 77 mole %, Cholesterol 20 mole %, and DOPE-PEG 3 mole %. Figure 1 shows the calcein release as a function of US exposure time.. Only after 0.5 min of exposure, already 20% of the calcein was released from DOPE-based liposomes. It is clear that for the formulations containing DOPE (full squares), the US sensitivity was dramatically increased with respect to an equivalent sample made of DOPC (full dots).

Inertial cavitation is generally accepted to induce leakage in lipid membranes and cell walls.²⁰ However, while it is evident that incorporation of DOPE lipids favors drug release, a clear understanding of the molecular mechanisms responsible for the increased sensitivity of PE-containing liposomes to ultrasound is at the present still lacking. This is mostly because it is extremely challenging to probe the formation of transient phase transitions, topologic transformations, or changes in curvature of lipid membranes as these perturbations are expected to self-heal in a time scale much faster than standard experimental techniques.

In this paper we investigated the effect of PE lipids on liposome membrane restructuring upon ultrasound exposure by utilizing two robust complementary techniques: Small Angle X-ray Scattering (SAXS) and Fluorescence Microscopy (FM). This enabled us to acquire a complete picture of liposome membrane sonosensitivity at different length scales. The time required for a lipid membrane phase transition or general perturbation is affected by the concentration of lipid as well as the viscosity of the solvent.²⁸ In order to evaluate the structural response of liposome solutions by FM, we promptly imaged liposomes after sonication in a sample where liposomes were dispersed in a highly viscous medium (Glycerol/Water). For SAXS measurements samples were analyzed quickly after ultrasound exposure in a highly concentrated regime.

SAXS measurements of DOPE-based liposomes before and after sonication

We used SAXS to investigate the details of structural changes of DOPE-based stealth liposomes induced by ultrasound energy. Figure 2A shows the SAXS diffraction patterns of DOPE-based liposomes (DOPE:DOPC:Cholesterol:DOPE-PEG; 30:47:20:3 mole%) at $\Phi_{\text{DOPE}}=0.3$ before (bottom black line) and after (top red line) sonication. Before any US energy is applied the samples showed three sharp reflections at the q vector positions of $q_{001}=0.065 \text{ \AA}^{-1}$, $q_{002}=0.13 \text{ \AA}^{-1}$, and $q_{003}=0.195 \text{ \AA}^{-1}$ resulting from a classic lamellar structure of lipid bilayers (L_{α}). The interlayer spacing can be calculated as $a = 2\pi/q_{001} = 96.7 \text{ \AA} = \delta_m + d_w$, where δ_m is the bilayer thickness and d_w is the size of the water layer. The bilayer thickness can be estimated from the equation $\delta_m \approx 1.6 l$, where l is the maximum length (nm) of a fully extended hydrocarbon chain. l can be also predicted by the equation $l = 0.15 + 0.127 n_c$,²⁹ where n_c is the total number of carbon atoms per chain. The estimated value for the membrane thickness δ_m is 40 Å leaving the thickness of water between bilayers d_w to be around 56 Å. This indicates that even though the SAXS experiments are conducted in a high concentration regime (1 M), there is still a considerable amount of water within the lipid bilayers and the system is far from being in a compact state. Two additional small reflections at $q_{11}=0.210 \text{ \AA}^{-1}$ and $q_{20}=0.252 \text{ \AA}^{-1}$ were also observed and are consistent with the presence of residual amounts of another phase. The q positions of these two peaks are correlated to an inverted hexagonal phase (H_{II}). It should be noted that the (10) reflection expected to the

hexagonal phase appears to be convoluted with the (002) peak for the lamellar phase. As a matter of fact a careful inspection of the (002) reflection in the lamellar phase reveals that this peak is asymmetric towards the lower q regime, most likely due to the presence a convoluted (10) peak characteristic of the H_{II} phase. The unit cell dimensions of H_{II} phases can be calculated as $a = 4\pi/[\sqrt{3}q_{11}] = 59.8 \text{ \AA}$. The SAXS diffraction peaks for sonicated DOPE-based liposomes at $\Phi_{\text{DOPE}}=0.3$, is presented in Fig. 2A, top red line. Two reflections at $q_{001}=0.073 \text{ \AA}^{-1}$ and $q_{002}=0.144 \text{ \AA}^{-1}$ are observed which indicates the presence of a lamellar phase of $a = 86 \text{ \AA}$ which corresponds to a reduction in lamellar spacing after sonication. Three other pronounced peaks at $q_{10} = 0.124 \text{ \AA}^{-1}$, $q_{11} = 0.215 \text{ \AA}^{-1}$, $q_{20} = 0.247 \text{ \AA}^{-1}$, are completely consistent with the coexistence of a H_{II} phase with lattice size dimensions of $a = 4\pi/[\sqrt{3}q_{10}] = 58.5 \text{ \AA}$.

DOPE-based liposomes at $\Phi_{\text{DOPE}}=0.62$ (DOPE:DOPC:Cholesterol:DOPE-PEG; 62:15:20:3 mole%) showed the similar trend to that obtained for liposomes at $\Phi_{\text{DOPE}}=0.30$. The SAXS scans obtained for unsonicated DOPE-based liposomes at $\Phi_{\text{DOPE}}=0.62$ are shown in Fig. 2B (bottom, black line). Five sharp reflections at $q_{001}=0.043 \text{ \AA}^{-1}$, $q_{002} = 0.0872 \text{ \AA}^{-1}$, $q_{003} = 0.131 \text{ \AA}^{-1}$, $q_{004} = 0.173 \text{ \AA}^{-1}$, $q_{005} = 0.217 \text{ \AA}^{-1}$, result from a lamellar phase with lattice spacing of $a = 2\pi/q_{001} = 146 \text{ \AA}$. This indicates that $\Phi_{\text{DOPE}}=0.62$ system contains more water than $\Phi_{\text{DOPE}}=0.30$. Also for this case, the lamellar phase is present in coexistence with a residual H_{II} phase with peaks at $q_{10} = 0.0774 \text{ \AA}^{-1}$, $q_{11} = 0.117 \text{ \AA}^{-1}$, and a lattice spacing of $a = 4\pi/[\sqrt{3}q_{10}] = 93.7 \text{ \AA}$. This spacing is considerably bigger than that obtained for $\Phi_{\text{DOPE}}=0.30$. From lattice spacing calculations, it can be concluded that higher DOPE content drives more water rich lipid phases. The SAXS results obtained for sonicated DOPE-based liposomes at $\Phi_{\text{DOPE}}=0.62$ are shown in Fig. 2B, top red line. The majority of observed peaks are consistent with the presence of a dominant H_{II} phase with peak positions at $q_{10} = 0.0725 \text{ \AA}^{-1}$, $q_{11} = 0.126 \text{ \AA}^{-1}$, $q_{20} = 0.141 \text{ \AA}^{-1}$ and unit cell dimensions of $a = 4\pi/[\sqrt{3}q_{10}] = 100 \text{ \AA}$. A residual lamellar phase can still be observed by the three weak peaks at $q_{001} = 0.0455 \text{ \AA}^{-1}$, $q_{002} = 0.0872 \text{ \AA}^{-1}$, $q_{005} = 0.215 \text{ \AA}^{-1}$, with unit cell dimensions of

$a = 2\pi/q_{001} = 138 \text{ \AA}$. These results show that DOPE containing liposomes mostly adopt a lamellar phase (L_α) before US is applied and the inverted hexagonal phase (H_{II}) after US is applied, as depicted schematically in Fig. 2, bottom right. This fact is most prominent for samples containing higher amounts of DOPE. As a reference state, liposomes containing all lipids except DOPE (DOPE:DOPC:Cholesterol:DOPE-PEG; 0:77:20:3 mole%, Fig. 2C) were measured by Synchrotron SAXS before (black line) and after (red line) ultrasound energy was applied. Except for the change in lamellar spacing as observed in the other systems, US is not capable of inducing membrane restructuring for systems where DOPE is not present. It should also be noted that for DOPE containing systems, there seems to be a significant form factor contribution to the SAXS signal in addition to the structure factor peaks. We consider out of the scope of this paper to clearly identify the origin of this signal but considering the q range at which it is present (*ca.* 30 \AA^{-1}) it is likely due to the presence of PEG-PE micelles in the bulk. Liposomes containing PEG-PE lipids are often observed in coexistence with PEG-PE based micelles in solution.³⁰

After 4 days, all samples were re-measured and it was observed that the sonicated concentrated lipid samples containing DOPE recovered into their original morphology displaying mostly lamellar phases. This corroborates that lipid membrane perturbations upon US exposure is expected to self-heal given enough time. At this point we did not conduct a careful time dependent study to evaluate the minimum required time for the systems to revert to the original structure before ultrasound exposure is employed.

FM studies of DOPE-based liposomes before and after sonication

We employed Fluorescence Microscopy to investigate the effect of sonication of stealth liposomes containing DOPE at the dilute regime. In order to be able to evaluate membrane structure rearrangements, the liposomes were prepared in a highly viscous environment where the time scale of defect formation and healing is significantly increased so observation by microscopy techniques is potentially possible. Figure 3 shows representative FM images of giant unilamellar vesicles (GUVs) of DOPE-based formulations at different compositions in the absence and presence of US energy. When the DOPE content is $\Phi_{\text{DOPE}} = 0.30$, we can observe that most GUVs are spherically shaped

vesicles with dimensions ranging from 1-10 μm as depicted in Fig. 3A. Figure 3B shows a DOPE based GUV at higher DOPE molar fractions ($\Phi_{\text{DOPE}}=0.62$). The vesicle is perfectly spherical but, most interestingly, the existence of long tubular protrusions of about $1\mu\text{m}$ in diameter can be observed growing out from the GUV membrane (white arrow in Fig. 3B). The presence of lipid tubes indicates that the lipid composition of this formulation with higher DOPE content is able to self-assemble into aggregates that deviate from the expected spherical shape.

After US treatment, both GUV samples displayed dramatically different structures. Figure 3C shows the system prepared with $\Phi_{\text{DOPE}}=0.30$ after 5 minutes exposure to US. The aggregates observed are on average considerably smaller (*ca.* 2 μm) than those obtained for the parent unsonicated system, the shapes of the aggregates are more diverse consisting of ellipsoidal and tubular structures (in addition to spheres), and the particles seem to be connected as in a pearl necklace configuration. A similar result is obtained to the system with higher DOPE content ($\Phi_{\text{DOPE}}=0.62$) presented in Fig. 3D except that the aggregates obtained after US exposure are an order of magnitude smaller (*ca.* 0.1 μm) than those obtained for sonicated $\Phi_{\text{DOPE}}=0.30$ samples. The “pearling” effect after US exposure can clearly be observed and shown on Fig. 3D inset with tens of μm long strings of connected sub-micron lipid vesicles. The general observation of the US effect on the GUVs is that the aggregate size is reduced. In addition, the smaller aggregates seem to be linked as in a pearl necklace configuration. This effect is observed for both DOPE containing samples but it is much more pronounced when the content of DOPE is higher. Pearling of GUVs in response to external stimuli has been previously investigated. Examples include nanoparticles adsorbed onto GUVs inner membrane leaflets mediating links between vesicles,³¹ polymer anchoring onto the membrane outer leaflet connecting aggregates,³² or under the stimulus of tension induced by optical tweezers.³³

Discussion

The effect of increasing amounts of DOPE ($\Phi_{\text{DOPE}}=0$, $\Phi_{\text{DOPE}}=0.30$, and $\Phi_{\text{DOPE}}=0.62$) on the sensitivity of stealth liposomal formulations to ultrasound energy comprising Cholesterol, DOPC, and DOPE-PEG was investigated by Small-Angle X-ray Scattering and Fluorescence Microscopy. Ultrasounds can lead to cavitation events that are known to provoke leakage of liposome membranes and cells in vitro as well as vivo.^{19,20} The exact mechanism responsible for membrane perturbation is still not clear but it may involve the formation of small pores induced by the bursting of air bubbles on membrane surfaces. Other effects that have been considered include temperature rising,¹² however membrane leakage induced by ultrasound is observed even when the average temperature is kept low. Another factor to consider is that increasing pressure leads to phase transformations in lipid systems,^{34,35} however, for DOPE based membranes at room temperature pressures of around 40 MPa are required for a transformation from a lamellar to reversed hexagonal phase.³⁶ The molecular mechanism associated with sonosensitivity of liposomes membranes might be a combination of many factors. In this paper we focus on membrane physico-chemical properties, in particular the effect of curvature stress. The inclusion of such local instabilities lowers the free energy cost associated with creating a pore in a membrane and thus the effect of inertial cavitation might be more pronounced in membranes that include components that perturb the average mean curvature of liposomal membranes. The main finding of this paper is that in the absence of DOPE the lipid membranes display the typical lamellar structure that remains stable upon ultrasound exposure and the only observation is reduction in bilayer spacing of about 10 Å. Changes in membrane thickness are often associated with a modification of the effective area per lipid head group. One example includes the increase in membrane thickness upon interaction with DNA that screens the electrostatic repulsion between the oppositely charged lipid head groups resulting in a smaller head group area and concomitant increase in the length occupied by the lipid tails.³⁷ In the case of lipid bilayers exposed to ultrasound, the thinning of the membrane could be explained by a higher mobility of lipid head groups at the bilayer/water interface, leading to an overall lowering of the membrane thickness as means to conserve lipid molecular volume. It should be noted that this

argument is consistent with the fact that the same degree (*ca.* 10 Å) of thinning of the membrane is observed for all three systems irrespective of amount of DOPE. The incorporation of DOPE in the lipid membranes promotes membrane restructuring upon ultrasound exposure and the dominant trend is the transformation of a lamellar phase into a reversed hexagonal structure that is most prevalent as the content of DOPE is increased. DOPE is a lipid with inversed conical molecular shape that is typically responsible for self-assembly into reverse structures (*e.g.* type II hexagonal- H_{II}) of negative preferred curvature $H < 0$. This property can be estimated by the “packing parameter”,³⁸ $P = V / (l \cdot A)$, where V is the volume of the hydrophobic portion of the surfactant molecules that can be estimated by the number of carbons in the chain ($V = 0.54 \text{ nm}^3$ for an 18 carbon chain length), l is the length of the hydrocarbon chains ($l = 2.4 \text{ nm}$ for a 18 carbon chain length), and A is the effective area per head group. The head group area of DOPC corresponds to $A_{\text{DOPC}} = 68.3 \text{ \AA}^2$ and that of DOPE equals $A_{\text{DOPE}} = 50 \text{ \AA}^2$,³⁹ taking into account the molar fractions of the systems ($\Phi_{\text{DOPE}}=0$, $\Phi_{\text{DOPE}}=0.30$, and $\Phi_{\text{DOPE}}=0.62$), the packing parameter without DOPE is close to unity ($P = 1.05$) as expected for lipids that prefer to assemble into flat bilayers. For the system with 30 mole % of DOPE, the packing parameter is raised above unity as predicted for molecules that tend to self-assemble into reversed structures ($P = 1.2$ for $\Phi_{\text{DOPE}}=0.30$ and $P = 1.4$ for $\Phi_{\text{DOPE}}=0.62$). It is clear that the incorporation of DOPE into a liposome formulation will induce local instabilities in the lipid bilayer membrane resulting in membrane restructuring upon an applied stress such as ultrasound energy. The transformation of the lamellar phase into a reversed hexagonal phase is characterized by the onset of membrane fusion and formation of pores which locally have negative curvature $H < 0$.²³ It should be noted that the hexagonal H_{II} phase is simply a collection of lipid tubes of the reverse type ($H < 0$, lipid molecule hydrocarbon chains pointing outwardly) concentrated and packed in a 2D hexagonal lattice. In the context of drug release, membrane instabilities that facilitate formation of reversed structures, *i.e.* pores, can be extremely beneficial, as perforations within the liposome membrane promoted by external stimuli will tremendously enhance drug permeation from the liposome aqueous interior to the exterior. This concept is depicted schematically in Fig. 4. It is our belief that the sonosensitivity of liposomal formulations relies on

this exact principle of membrane instabilities such as the insertion of DOPE, an intrinsically negative curvature lipid ($H < 0$), embedded in a flat, zero curvature ($H = 0$) liposomal membrane. These instabilities nucleate and propagate as energy (*i.e.* ultrasound) is applied to the system resulting in membrane restructuring such as the formation of pores and/or tubular aggregates. In addition to the membrane local phase transformations, the fact that we observed that membranes after ultrasound become thinner should also add to the enhanced permeability of drugs through liposomal membranes upon ultrasound exposure, even without any formation of pores. In addition, the bending rigidity κ of lipid membranes display a quadratic scaling with the membrane thickness δ_m ($\kappa \propto \delta_m^2$)⁴⁰ hence one can expect the liposome membranes to be easier to bend after ultrasound energy has been applied.

The content of DOPE should be kept at moderate levels so that the membrane instabilities are only stimulated upon external stimuli or else one can expect excessive leakage and poor shelf-life stability of the formulations. In fact, our fluorescence microscopy investigations within the dilute regime using GUVs at different molar fractions of DOPE indicate that even before any ultrasound energy is applied, the GUVs with molar fractions of DOPE as high as $\Phi_{\text{DOPE}}=0.62$ already display the presence of other structures in addition to the regular flat liposome membrane. Long tubular structures protruding out of the GUV membrane are readily noted in Fig. 3B. This result completely corroborates the SAXS data where before US is applied to the concentrated lipid system with $\Phi_{\text{DOPE}}=0.62$, non-lamellar phases such as inverted lipid tubules packed in a 2D hexagonal array- H_{II} , are clearly coexisting with the flat bilayer lamellar phase- L_{α} .

In the dilute regime, our results shown in Fig. 3 indicate that the general structural response of GUVs containing DOPE to ultrasound is essentially the formation of much smaller aggregates mediated by the recognized phenomenon of GUV pearling. Smaller aggregates of diverse shapes are stringed together as in a pearl-necklace configuration. The main difference that higher amounts of DOPE ($\Phi_{\text{DOPE}}=0.62$) confer to the system is essentially the bead-size of the pearl-necklace structure to be dramatically smaller when compared to what is obtained for $\Phi_{\text{DOPE}}=0.30$. It should be noted that these formulations contain 20 moles% of cholesterol (as most liposome formulations do in

pharmacological applications). Cholesterol has been recognized for decades to induce lateral segregations within the membrane.⁴¹⁻⁴³ The domains are often called lipid rafts and refer to uneven molecular mixing of the bilayer with particular lipid species segregated in domains that will have different mobility, ordering, and elasticity compared to the rest of the membrane. Fluorescence microscopy is a useful technology to observe raft formation in GUVs⁴⁴ and the most popular lipid composition yielding lipid segregation is the inclusion of Cholesterol and sphingomyelin (SMP) in combination with a variety of phospholipids including DOPE:DOPC based.⁴⁵ However, cholesterol is known to promote segregation of liquid ordered and liquid disordered domains for lipid bilayers in general^{43, 46} and rafts have been reported to exist and have specific functions in real molecularly diverse biological membranes.⁴⁷ In a more general sense, lipid segregation is strongly related with liposome self-assembly and it has been suggested that non-spherical vesicles observed in certain lipid systems comprise membranes where lipids demix and reorganize according to preferred mean curvature (with rectangular shaped lipids concentrated in the flat lipid membranes and conically shaped lipids gathering at the tubular membrane domains). This curvature-driven lipid sorting into populations is based on a balance of relative energy (bending, mixing entropy, and interactions between species) costs of forming bent membranes at thermal equilibrium.⁴⁸ There is currently strong evidence that this lipid reorganization is the underlying mechanism of highly curved transport intermediates in cells; for example, tubules emerging from endosomes⁴⁹ and vesicle budding from the Golgi apparatus⁵⁰ both show different lipid compositions than from where they stemmed. In light of these findings, it is conceivable that the DOPE molecules in the GUV membranes are also sorted according to preferred mean curvature and the tubular protrusions observed in GUVs at $\Phi_{\text{DOPE}}=0.62$ depicted in Fig. 3B are most likely DOPE rich. Figure 5A shows the image of a GUV at $\Phi_{\text{DOPE}}=0.30$ before ultrasound energy is applied. We can observe that the lipid membrane region is not perfectly homogeneous indicating that different domains or lateral lipid segregations may indeed be present. At this point we cannot identify if these domains are simply liquid ordered/liquid disordered rafts promoted by the presence of cholesterol and/or curvature induced lipid sorting. In any case, when ultrasound energy is applied to such system one observes a transition of the GUV into smaller

aggregates connected in a string (commonly referred as vesicle pearling), which is likely initiated at these domains or membrane instabilities. A schematic representation of the pearling mechanism is depicted in Fig. 5B. It should also be noted that we established by SAXS that ultrasound induces thinning of the lipid membrane rendering it more likely to bend. The higher the DOPE content the lower the elastic free energy of the membrane is and GUV pearling should occur easier. Consequently we observe that for GUVs with $\Phi_{\text{DOPE}}=0.62$ the aggregates undergo higher degree of pearling resulting in the formation of considerably smaller aggregates when compared to GUVs containing the intermediate DOPE content ($\Phi_{\text{DOPE}}=0.30$).

Conclusions

Small Angle X-ray Scattering and Fluorescence Microscopy techniques were employed to carefully investigate the structural evolution of liposomal membranes in response to ultrasound for a number of formulations intended for triggered drug delivery. The objective of this work was to investigate the sensitivity of liposomes to acoustic energy when they are doped with additives that perturb the lipid packing within the bilayer of the liposome membrane. We studied the effect of adding components that are able to modify the elastic free energy of the membrane by incorporation of DOPE lipids with intrinsic preferred negative curvature that promote topological transformations from flat to perforated membranes from where drugs can readily permeate out the liposomal carrier.

The response of the liposomal membrane to acoustic energy depends on the amount of the “non-lamellar” lipid additive (DOPE). When DOPE is absent, the liposomal membrane displays a clear lamellar phase L_{α} with (001), (002), and (003) SAXS reflections that responds to ultrasound by thinning *ca.* 10 Å. When DOPE is raised to intermediate fractions of 30 mole % the membranes remain mostly in their original lamellar L_{α} state, but exposure to ultrasound promotes restructuring and the rise of a reversed hexagonal phase (H_{II}). This can clearly be detected by the SAXS (10), (11), and (20) reflections. When DOPE contents are as high as 62 mole %, the membrane shows signs of the presence of non-lamellar phases (H_{II}) even prior to ultrasound exposure. We argue that the inclusion of non-lamellar forming lipids induces instabilities in the liposome membrane, lowering the elastic free energy of the system rendering the bilayer more bendable as well as more prone to experience topological phase transitions. In the dilute regime, Giant Unilamellar Vesicles observed by Fluorescence microscopy reveal that at high contents of DOPE (62 mole %) the system is composed of spherical vesicles in combination with tubular structures, indicating that there might be curvature-driven lipid sorting in the liposomal membranes where DOPE would be most likely localized to the tubular domains of negative curvature. In response to ultrasound, the GUVs displayed a transition to a pearl-necklace like configuration. We argue that the onset of pearling is initiated at sites of curvature stress comprising DOPE membrane domains. Our work gives a fundamental understanding for the mechanism of the lipid membrane restructuring upon US

exposure, providing useful guidelines for the design of sonosensitive liposomes for targeted drug delivery applications.

Acknowledgments

This work was supported by start-up funding from the University of Illinois at Urbana-Champaign, College of Engineering. We acknowledge the assistance of Adam and Kejia in generating and observing GUVs.

Figure Captions

Figure 1. Calcein release (%) from liposomes measured by fluorescence. The full squares are for a sample containing $\Phi_{PE}=0.62$ (DOPE:DOPC:Cholesterol:DOPE-PEG; 62:15:20:3 mole%). The full dots are for a sample containing $\Phi_{PE}=0$ (DOPE:DOPC:Cholesterol:DOPE-PEG; 0:77:20:3 mole%). Liposomes containing DOPE are much more responsive to US during the time range of exposure.

Figure 2. Small angle X-ray scattering (SAXS) data obtained for DOPE-based liposomes at (A) $\Phi_{PE}=0.3$ (DOPE:DOPC:Cholesterol:DOPE-PEG; 30:47:20:3 mole%) (B) $\Phi_{PE}=0.62$ (DOPE:DOPC:Cholesterol:DOPE-PEG; 62:15:20:3 mole%) (C) $\Phi_{PE}=0$ (DOPE:DOPC:Cholesterol:DOPE-PEG; 0:77:20:3 mole%) before US treatment (bottom black line) and after US treatment (top red line). DOPE-based liposomes (A, B) mostly adopt a lamellar phase before US energy is applied and after US treatment, an inverted hexagonal phase (HII) becomes the dominant phase for both cases. Reference liposomes (C) which do not contain DOPE only show a lamellar phase that responds to US treatment by thinning ca. 10 Å. This indicates that DOPE lipids are responsible for HII phase appearance in DOPE-containing liposomes (A, B).

Figure 3. Fluorescence images of giant unilamellar vesicles (GUVs) of DOPE-based liposomes at (A) $\Phi_{PE}=0.3$ before US treatment (B) $\Phi_{PE}=0.62$ before US treatment (C) $\Phi_{PE}=0.3$ after US treatment (D) $\Phi_{PE}=0.62$ after US treatment. Liposomes before US treatment (A, B) are mostly spherical but for higher contents of DOPE, tubular aggregates are present as well as indicated by the white arrow. After US treatment, liposomes (C, D) restructure into small vesicles that are connected several μm long strings, a phenomena well known as GUV pearling. Scale bars = 3 μm .

Figure 4. Illustration of the proposed mechanism for the restructuring of DOPE-based liposomal membranes upon ultrasound stimuli. The incorporation of DOPE within the flat liposomal membrane ($H = 0$) is a source of negative curvature ($H < 0$) stresses that lower the membrane elastic free energy of the system. When US energy is applied, the membrane system responds by a topological phase transition where pores with local negative membrane curvature ($H < 0$) are generated. This will lead to rapid permeation of small drugs from the liposome interior.

Figure 5. (A) To the left: image of a giant unilamellar vesicle (GUV) at $\Phi_{\text{DOPE}}=0.30$ before ultrasound exposure is applied, which shows an inhomogeneous lipid membrane suggesting the existence of lipid membrane segregations. To the right: suggested lipid domain formation based on curvature-driven lipid sorting with DOPE rich (red) regions of negative curvature embedded in DOPC of zero mean curvature (blue). (B) Schematic illustration of the shape change in GUVs upon ultrasound stimuli. DOPE rich regions of higher curvature promote the onset of GUV pearling. The higher the DOPE content, the easier it is to bend the membrane and pearling leads to the transformation of the GUVs into much smaller aggregates when compared to intermediate contents of DOPE.

References

1. C. P. McCoy, C. Brady, J. F. Cowley, S. M. McGlinchey, N. McGoldrick, D. J. Kinnear, G. P. Andrews and D. S. Jones, *Expert opinion on drug delivery*, 2010, 7, 605–616.
2. S. Mura, J. Nicolas and P. Couvreur, *Nat. Mater.*, 2013, 12, 991–1003.
3. A. Schroeder, R. Honenb, K. Turjemanb, A. Gabizonc, J. Kosta and Y. Barenholz, *J. Control. Release*, 2009, 137, 63–68.
4. A. Kheirloom, L. M. Mahakian, C.-Y. Lai, H. A. Lindfors, J. W. Seo, E. E. Paoli, K. D. Watson, E. M. Haynam, E. S. Ingham, L. Xing, R. H. Cheng, A. D. Borowsky, R. D. Cardiff and K. W. Ferrara, *Mol. Pharm.*, 2010, 7, 1948–1958.
5. S. Qin, C. F. Caskey and K. W. Ferrara, *Physics in medicine and biology*, 2009, 54, R27–57.
6. C. H. Wang, S. T. Kang, Y. H. Lee, Y. L. Luo, Y. F. Huang and C. K. Yeh, *Biomaterials*, 2012, 33, 1939–1947.
7. M. Javadi, W. G. Pitt, D. M. Belnap, N. H. Tsosie and J. M. Hartley, *Langmuir*, 2012, 41, 14720–14729.
8. G. L. Britton, H. Kim, P. H. Kee, J. Aronowski, C. K. Holland, D. D. McPherson and S. L. Huang, *Circulation*, 2010, 122, 1578–1587.
9. Y. Negishi, D. Omata, H. Iijima, Y. Takabayashi, K. Suzuki, Y. Endo, R. Suzuki, K. Maruyama, M. Nomizu and Y. Aramaki, *Mol. Pharm.*, 2010, 7, 217–226.
10. Y. Negishi, Y. Endo-Takahashi, Y. Matsuki, Y. Kato, N. Takagi, R. Suzuki, K. Maruyama and Y. Aramaki, *Mol. Pharm.*, 2012, 9, 1834–1840.
11. K. Un, S. Kawakami, R. Suzuki, K. Maruyama, F. Yamashita and M. Hashida, *Mol. Pharm.*, 2011, 8, 543–554.
12. A. Schroeder, Y. Avnir, S. Weisman, Y. Najajreh, A. Gabizon, Y. Talmon, J. Kost and Y. Barenholz, *Langmuir*, 2007, 23, 4019–4025.
13. I. Y. Kim, Y. S. Kang, D. S. Lee, H. J. Park, E. K. Choi, Y. K. Oh, H. J. Son and J. S. Kim, *J. Control. Release*, 2009, 140, 55–60.
14. C. Leal, N. F. Bouxsein, K. K. Ewert and C. R. Safinya, *J. Am. Chem. Soc.*, 2010, 132, 16841–16847.
15. C. Leal, K. K. Ewert, R. S. Shirazi, N. F. Bouxsein and C. R. Safinya, *Langmuir*, 2011, 27, 7691–7697.
16. C. Leal, K. S. Rognvaldsson, S. L. Fossheim, E. A. Nilssen, T. J. Evjen, Acoustically sensitive drug delivery particles comprising non-lamellar forming lipids, Norway patent # 8765172, 2012.
17. C. Leal, K. S. Rognvaldsson, S. L. Fossheim, E. A. Nilssen, Use of Particles comprising an alcohol, Norway pending # 20110020429, 2011.
18. M. A. Tran, R. Gowda, A. Sharma, E. J. Park, J. Adair, M. Kester, N. B. Smith and G. P. Robertson, *Cancer Res.*, 2008, 68, 7638–7649.
19. S. M. Graham, R. Carlisle, J. J. Choi, M. Stevenson, A. R. Shah, R. S. Myers, K. Fisher, M. B. Peregrino, L. Seymour and C. C. Coussios, *J. Control. Release*, 2014, 178, 101–107.
20. V. Frenkle, *Adv. Drug Deliv. Rev.*, 2008, 60, 1193–1208.
21. S. M. Gruner, P. R. Cullis, M. J. Hope and C. P. Tilcock, *Annu. Rev. Biophys. Biophys. Chem.*, 1985, 14, 211–238.
22. R. N. Lewis, D. A. Mannoock, R. N. McElhaney, D. C. Turner and S. M. Gruner, *Biochemistry*, 1989, 28, 541–548.
23. J. M. Seddon, *Biochim. Biophys. Acta*, 1990, 1031, 1–69.
24. H. Y. Lin and J. L. Thomas, *Langmuir*, 2003, 19, 1098–1105.
25. T. J. Evjen, E. A. Nilssen, S. Barnert, R. Schubert, M. Brandl and S. L. Fossheim, *European journal of pharmaceutical sciences : official journal of the European Federation for Pharmaceutical Sciences*, 2011, 42, 380–386.
26. D. D. Lasic, *Liposomes from Physics to Applications*, Elsevier Amsterdam, 1993.
27. M. I. Angelova, S. Soléau, P. Méléard, F. Faucon and P. Bothorel, *Preparation of giant vesicles by external AC electric fields. Kinetics and applications*, Steinkopff, 1992.

28. O. Sandre, L. Moreaux and F. Brochard-Wyart, *Proc. Natl. Acad. Sci. U.S.A.*, 1999, 96, 10591–10596.
29. D. F. E. a. H. Wennerström, *THE COLLOIDAL DOMAIN*, 2 edn., Wiley-VCH, 1999.
30. C. Leal, S. Rognvaldsson, S. Fossheim, E. A. Nilssen and D. Topgaard, *J. Coll. Int. Sci.*, 2008, 325, 485-493.
31. Y. Yu and S. Granick, *J. Am. Chem. Soc.*, 2009, 131, 14158–14159.
32. I. Tsafrir, D. Sagi, T. Arzi, M. A. Guedeau-Boudeville, V. Frette, D. Kandel and J. Stavans, *Physical review letters*, 2001, 86, 1138-1141.
33. R. Bar-Ziv, E. Moses and P. Nelson, *Biophysical journal*, 1998, 75, 294–320.
34. K. P. Shaw, N. J. Brooks, J. A. Clarke, O. Ces, J. M. Seddon and R. V. Law, *Soft Matter*, 2012, 8, 1070-1078.
35. N. J. Brooks, O. Ces, R. H. Templer and J. M. Seddon, *Chem. Phys. Lipids*, 2011, 164, 89–98.
36. J. Erbes, A. Gabke, G. Rapp and R. Winter, *Phys Chem Chem Phys.*, 1999, 2, 151–162.
37. C. Leal, D. Sandstrom, P. Nevsten and D. Topgaard, *Biochim. Biophys. Acta*, 2008, 1778, 214-228.
38. J. N. Israelachvili, D. J. Mitchell and B. W. Ninham, *J. Chem. Soc., Faraday Trans. 2*, 1976, 72, 1525-1568.
39. D. Marsh, *Biophysical journal*, 1997, 72, 2834–2836.
40. R. Goetz, G. Gompper and R. Lipowsky, *Phys. Rev. Lett.*, 1999, 82, 221–224.
41. J. R. Silvius, *Biochim. Biophys. Acta*, 2003, 1610, 174–183.
42. D. Lingwood and K. Simons, *Science*, 2010, 327, 46–50.
43. J. H. Ipsen, G. Karlström, O. G. Mouritsen, H. Wennerström and M. J. Zuckermann, *Biochim. Biophys. Acta*, 1987, 905, 162–172.
44. O. Wesołowska, K. Michalak, J. Maniewska and A. B. Hendrich, *Acta Biochim. Pol.*, 2009, 56, 33–39.
45. A. V. Samsonov, I. Mihalyov and C. F. S., *Biophys. J.*, 2001, 81, 1486–1500.
46. T. Baumgart, S. Hess and W. Webb, *Nature*, 2003, 425, 821–824.
47. G. van Meer, D. R. Voelker and G. W. Feigenson, *Nat. Rev. Mol. Cell Biol.*, 2008, 9, 112–124.
48. A. Callan-Jones, B. Sorre and P. Bassereau, *Cold Spring Harbor perspectives in biology*, 2011, 3, a0046–0048.
49. S. Mukherjee and F. R. Maxfield, *Traffic*, 2000, 1, 203–211.
50. R. W. Klemm, C. S. Ejsing, M. A. Surma, H. J. Kaiser, M. J. Gerl, J. L. Sampaio, Q. de Robillard, C. Ferguson, T. J. Proszynski, A. Shevchenko and K. Simons, *J. Cell Biol.*, 2009, 185, 601–612.

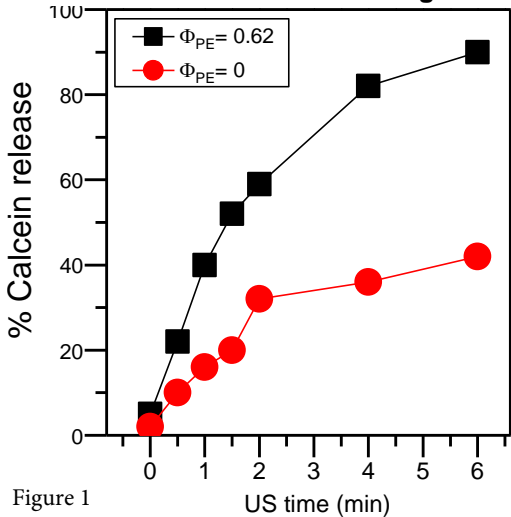


Figure 1

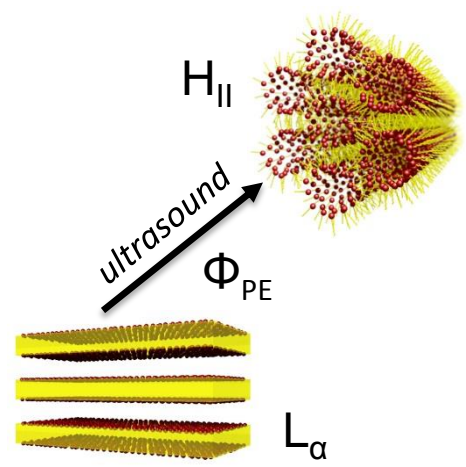
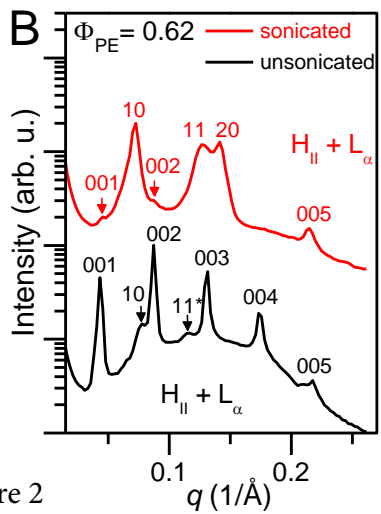
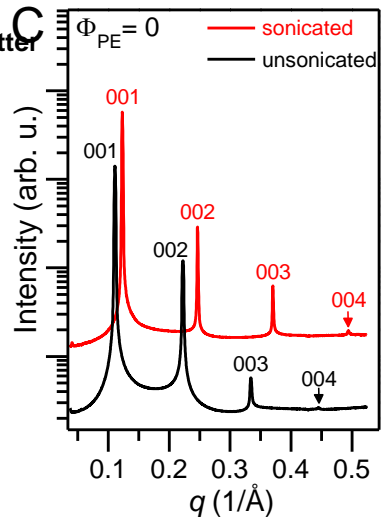
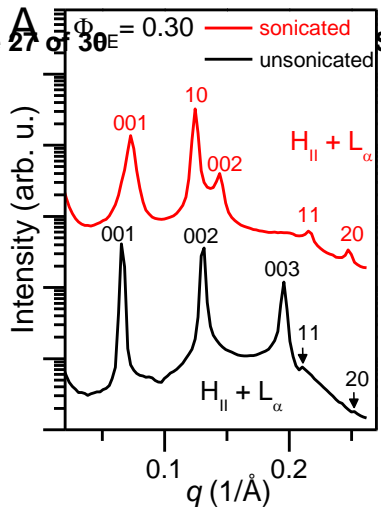
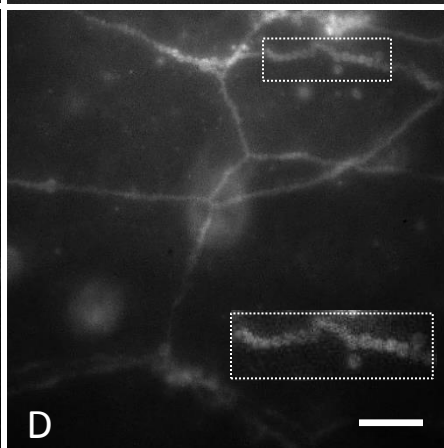
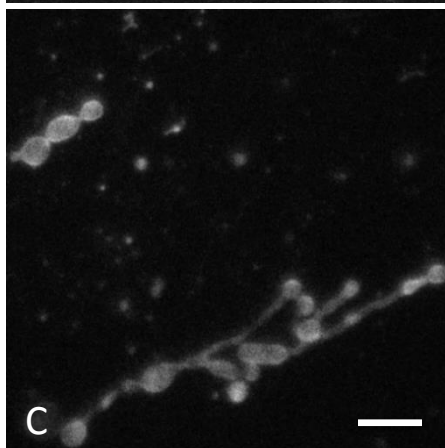
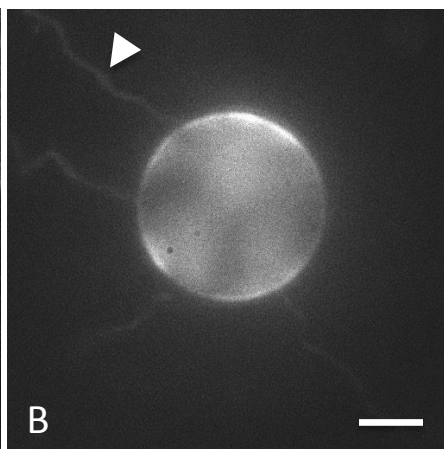
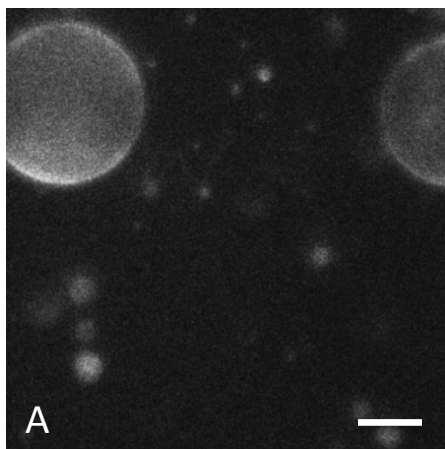


Figure 2

$\Phi_{PE}=0.30$

Soft Matter $\Phi_{PE}=0.62$

Page 28 of 30



Before US energy

Soft Matter Accepted Manuscript

After US energy

Figure 3

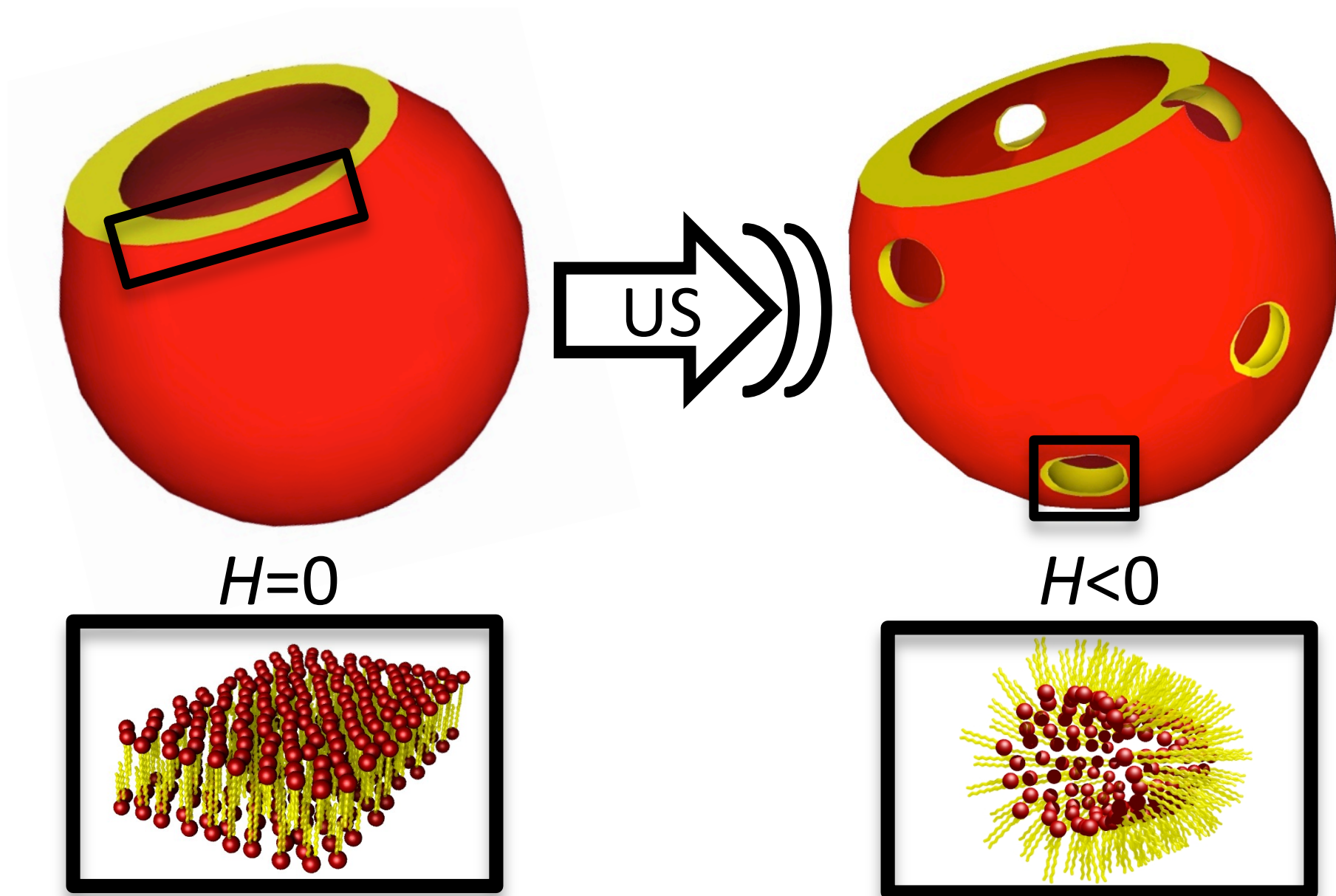


Figure 4

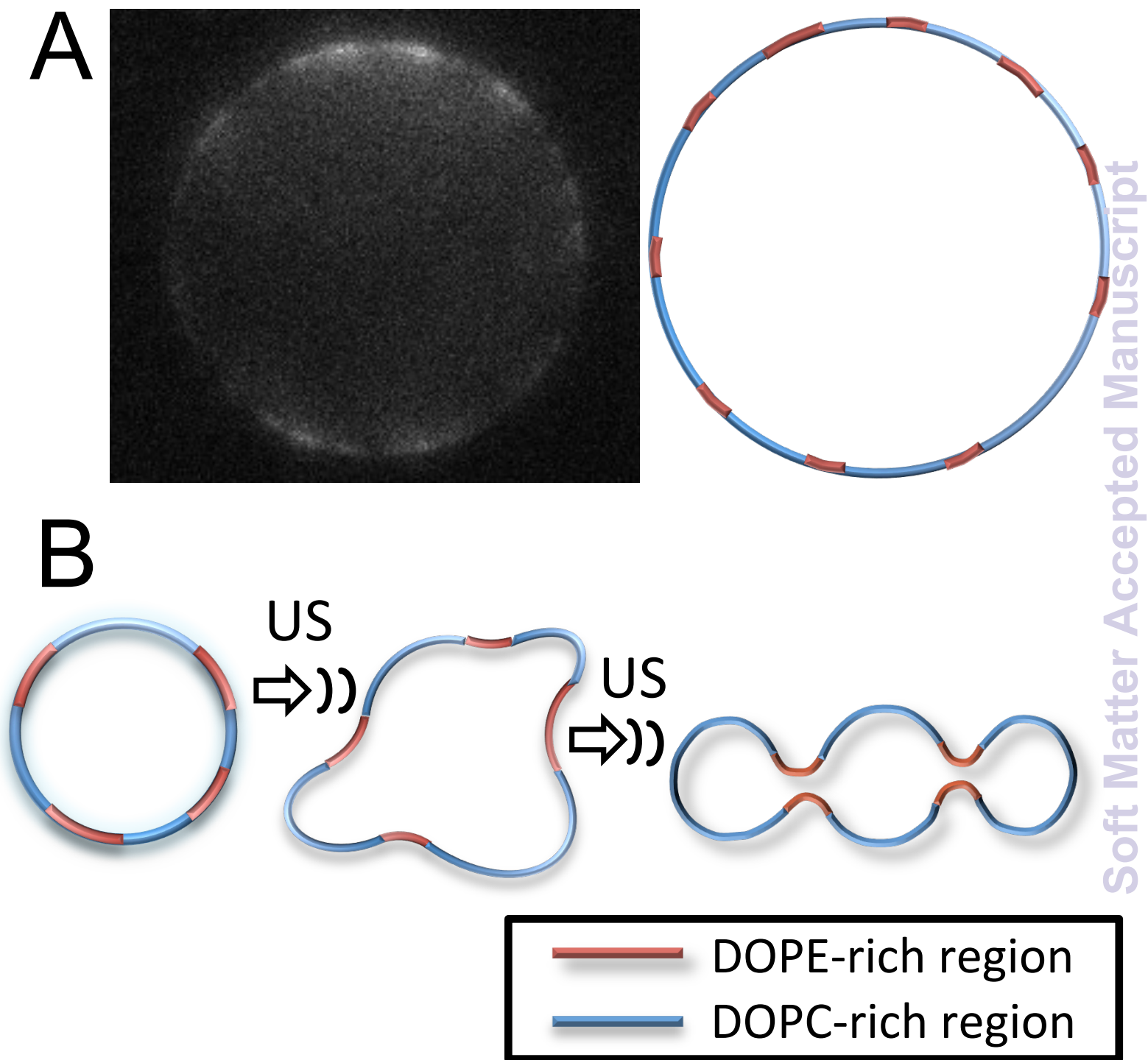


Figure 5